Understanding Regional Dynamics

Minoru Osawa

Institute of Economic Research, Kyoto University

osawa.minoru@gmail.com

September 18, 2025

Preliminary Work

The title and contents can change drastically.

Can dynamic forces of agglomeration generate spatial diversity, or do they inevitably concentrate activity into a single core? We investigate the theoretical properties of Allen and Donaldson (2020) model, a dynamic spatial framework featuring inter-generational externalities and endogenous migration. In a stylized multi-region economy, we show that the model yields stable equilibrium paths only under single-core agglomeration, closely echoing its static counterpart, the Allen and Arkolakis (2014) model. Although oscillatory dynamics can, in theory, produce multi-centered outcomes, such fluctuations may be less empirically plausible. Our results point to a key challenge: how to reconcile dynamic stability with polycentric spatial patterns observed in the real world?

Keywords: Quantitative spatial models, interregional transport, dynamics, agglomeration, economic geography.

JEL Classification: F15, R12.

I thank Takanori Ago and Tomoya Mori for their comments. Financial support from JSPS KAKENHI Grant Number JP22K04353 is warmly acknowledged.

1 Introduction

Long-run evaluation of regional and urban policies is essential for addressing inequality, demographic change, and the resilience of local economies. To provide credible guidance, spatial models need to account not only for the cross-sectional distribution of economic activity but also for the dynamic interplay between agglomeration and dispersion forces over time. A central mechanism is the feedback loop in which greater urban attractiveness draws more population, whose presence further enhances productivity and amenities. Such processes can sustain growth but also deepen fragility when fundamentals are weak.

Allen and Donaldson (2020) (henceforth AD) proposed a tractable dynamic regional model that extends the static framework of Allen and Arkolakis (2014) (henceforth AA) by incorporating forward-looking migration as well as intergenerational agglomeration externalities. The model has since been applied to a range of empirical settings. However, the theoretical implications of the AD framework on "endogenous" spatial structure remain underexplored.

Endogenous spatial structures, or *ex post* regional asymmetries from *ex ante* symmetric environments have been the main fascination of the economics of agglomeration (Fujita and Thisse, 2013) after the seminal work of Krugman (1991). In this literature, discussions have centered around how "endogenous" agglomeration and dispersion forces mediated by various types of transport frictions can shape uneven spatial distribution of mobile factors (Proost and Thisse, 2019). Here, "endogenous" forces, refer to all effects of the location of economic agents relative to one another, or the "second nature" of Krugman (1993).

Crucially, it has been recognized in this literature that *which* endogenous dispersion mechanism a model embeds is not an innocuous choice as it can flip the qualitative sign of policy counterfactuals. In static two-region spatial equilibrium models, the effect of transport policy depends on the dominant dispersion force. In Helpman (1998)-type settings (including AA) that emphasize local congestion externalities *within* each location, lower trade costs shift population toward peripheral areas. Here, transport infrastructure acts as an equalizing force. By contrast, in Krugman (1991)-type frameworks in which immobile factors combined with market crowding produces a dispersion force *across* locations, the same policy can intensify concentration. This occurs through the "siphoning" effect, where improved links draw activity from peripheral regions into core hubs, harming lagging regions.

Figure 2 illustrates the difference between the two types of models in symmet-

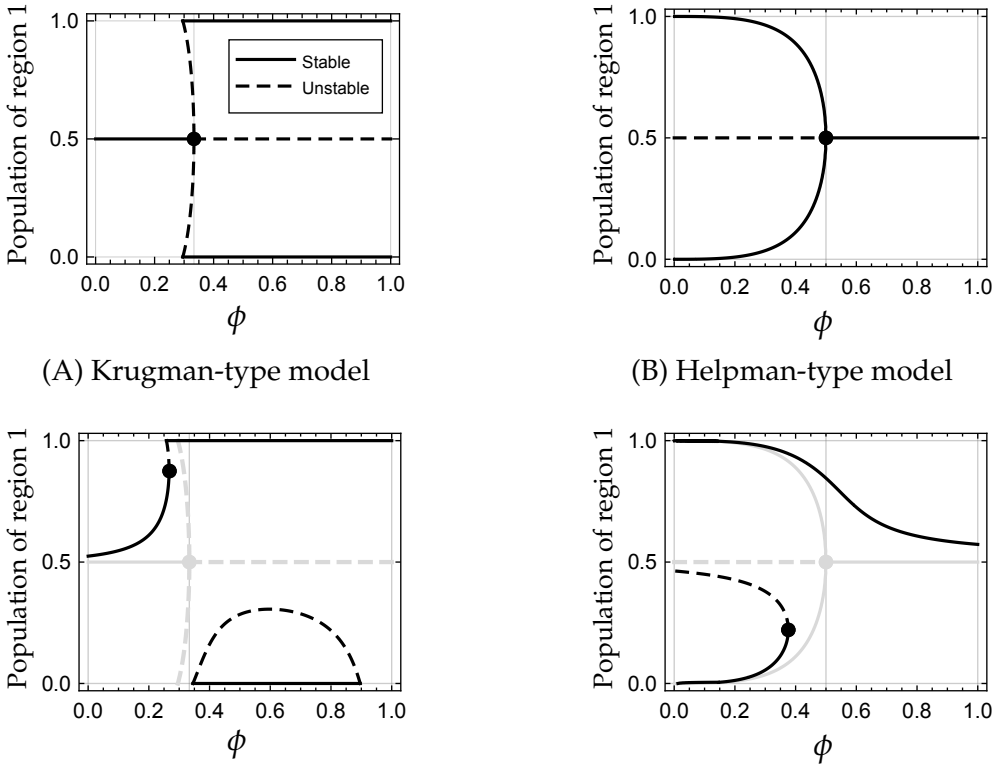

(A) Krugman-type model

(B) Helpman-type model

(C) Krugman-type model with asymmetry

(D) Helpman-type model with asymmetry

Figure 1: Spatial equilibria in Krugman- and Helpman-type frameworks

Note: A stylized two-region example. Figures taken from Akamatsu et al. (2024). The horizontal axis $\phi \in (0,1)$ denotes the trade freeness, with 0 indicating autarky and 1 indicating free trade.

ric and asymmetric two-region settings. Agglomeration occurs if transport costs are high (ϕ small) in the Krugman-type model (Fig. 1A), and the converse is true for the Helpman-type model (Fig. 1B). The qualitative contrast does not disappear even when asymmetries in exogenous fundamentals are present (Figs. 1C and 1D).

These interpretative tensions can be amplified in dynamic contexts, especially when inter-generational externalities are present. Short-run gains can be dampened, amplified, or even reversed as future cohorts endogenously adjust their location decisions. Clarifying the conditions under which each mechanism prevails is essential, as this can substantially affect the interpretation of policy outcomes in quantitative exercises.

This study takes a step toward clarifying these dynamics by analyzing the equilibrium structure of the AD model in a stylized setting. Following the agenda the author proposed in Akamatsu et al. (2017, 2024), we analyze a stylized multi-location version of the AD model on a circular geography to distill the workings of endogenous forces. Our contributions are the following:

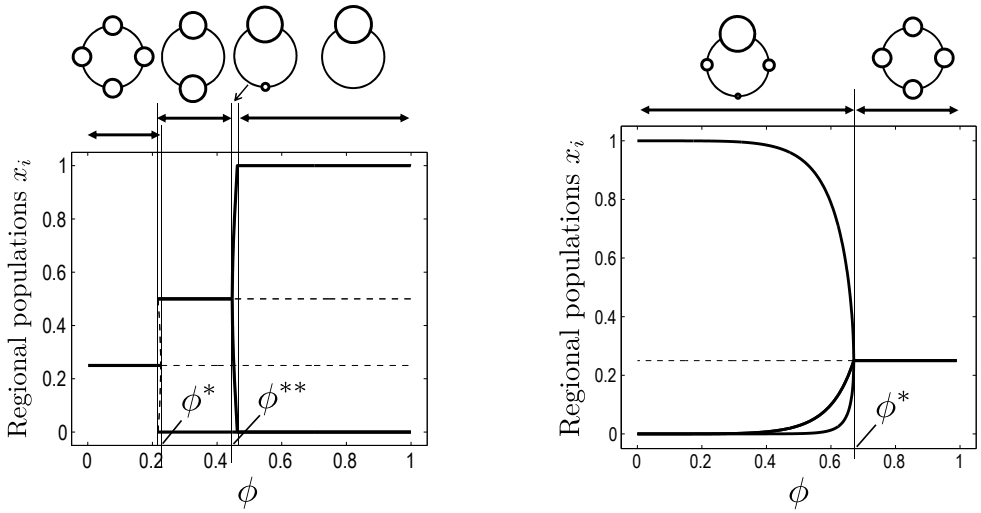

(A) Krugman-type model (B) Helpman-type model

Figure 2: Spatial distributions in a symmetric four-region economy.

1. We derive closed-form conditions in the space of two policy-relevant parameters: the iceberg trade-cost index and the elasticity of interregional migration ("migration resistance");

2. We show that, outside knife-edge cases, the AD model either behaves like its static AA counterpart, or generates oscillations in city sizes, which would be less relevant in reality.

While simplified by design, this analysis helps clarify how dynamic feedbacks interact with dispersion forces to shape long-run spatial configurations. Our findings suggest that the introduction of inter-generational externalities and migration dynamics alone does not fundamentally alter the qualitative behavior of static models, unless one is willing to tolerate less plausible oscillatory outcomes. This highlights the remaining importance of theoretical groundwork of spatial models, especially for applied policy evaluation in environments undergoing rapid structural change.

This study is motivated by Akamatsu et al. (2017, 2024), which emphasizes the distinction between dispersion forces that act *within* locations and those that arise *across* them. Specifically, we can theoretically identify two types of dispersion forces:

- *Local dispersion force* (Helpman-type dispersion mechanisms) stems from congestion *within* each location. The representative origin of such forces is the inelastic supply of land. Because it intensifies with point-wise pop-

(A) Krugnam-type model (B) Helpman-type model

Figure 3: Spatial distributions in a square economy with uniform fundamentals.

ulation density, lowering transport costs increases its relative importance and hence foster local spreading of economic agglomerations.

- *Global dispersion forces* (Krugman-type dispersion mechanisms) originates from market crowding *across* space combined with immobile factors. Each agglomeration casts a geographical "shadow" that repels rivals (cf. Hornbeck et al., 2024), promoting multi-centric patterns.

In particular, in multi-location settings beyond two, the two mechanisms imply qualitatively different spatial implications. For illustration, Figure 2 compares a Krugnam-type model and a Helpman-type model in a symmetric four-location circle, where the horizontal axis is the freeness of trade. Multiple cores can emerge only in the former, whereas the latter features only a single-peaked spatial distributions. This qualitative difference persist even when we consider two-dimension setting (Fig. 3).

Because both dispersion mechanisms operate in reality, a model that emphasize only one may risk misleading policy prescriptions. As a quantitative example, Figure 4 from Sugimoto et al. (2025) illustrates the observed and counterfactual population changes across Japanese regions, with a focus on the long-run impact of highway infrastructure. Panels (A) and (B) simulate the counterfactual scenario in which highways are removed (i.e., transport costs go up), based on a plain Helpman-type model and a Helpman-type plus Krugman-type dispersion mechanism, respectively. While neither model fully reproduces the actual evolution of Japanese population patterns, a striking contrast emerges between the two counterfactual scenarios. In (A), there is a concentration toward the core when highways are removed. This is broadly consistent with Fig. 1B when transport cost goes up (ϕ decreases), but somewhat contradicts to the actual phenomena in the past decades in Japan. In contrast, in (B), which combines both local and global dispersion forces, yields the opposite result: the same removal of highways induces a population shift toward peripheral regions. This qualitative reversal illustrates how the nature and composition of dispersion forces can

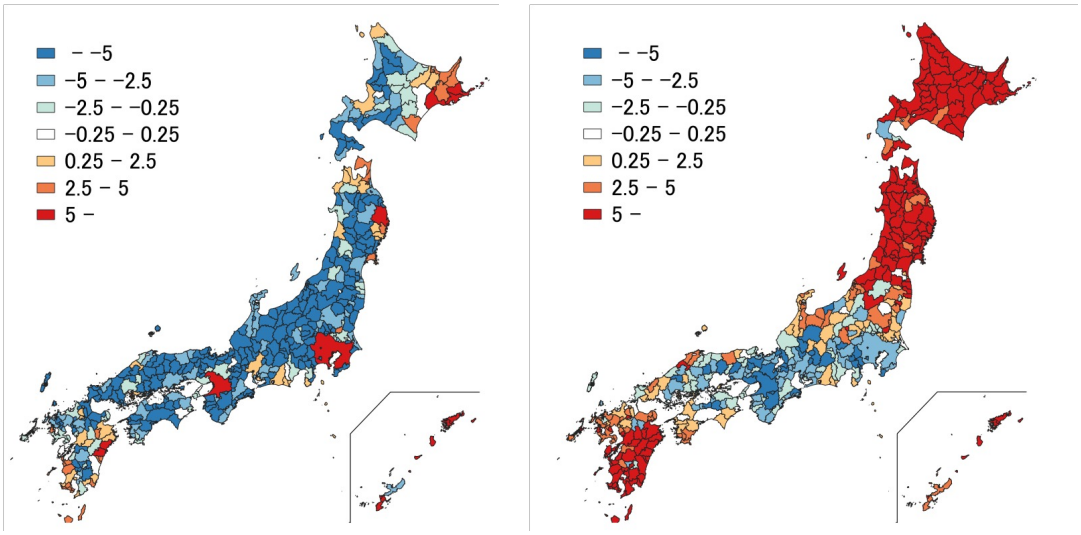

(A) Helpman-type (B) Helpman + Krugman

Figure 4: Counterfactual population changes of Japanese regions under counterfactual removal of highways (reproduced from Sugimoto et al. (2025)).

fundamentally shape counterfactual outcomes in quantitative spatial models.

Without exogenous heterogeneity, Helpman-type frameworks do not generate polycentric equilibria nor concentration towards the core when transport costs fall. The present study reveals that this property persists in the AD framework, a dynamic version of the AA framework. The agglomeration behavior we obtain for the dynamic framework by AD resembles static Helpman-type frameworks in which stable agglomeration pattern features only mono-centric configurations.

2 The AD Model

For self-containedness, the AD framework is briefly summarized below. One can just skip this section if they are familiar with the framework.

Basic settings. Consider a finite set of *locations* $\mathcal{N} \equiv \{1, 2, \ldots, N\}$ and discrete time periods $t = 0, 1, 2, \ldots$. Unless otherwise noted, variables without the time index is interpreted to belong to period t.

A continuum of homogeneous agents (i.e., workers/consumers) exists in this economy. Each agent lives for two periods: a youth period and an adulthood period. Only adult consumers engage in consumption and labor supply. In their adulthood, each consumer supplies one unit of labor inelastically. At every point in time, we normalize the total number of adult consumers to $L > 0$.

Alternatively, we assume that upon exiting the economy, each cohort of adult consumers is immediately replaced by the same number of young consumers, who are newly born across all locations. An interesting model that accounts for fertility dynamics is discussed in Allen and Donaldson (2022).

Let L_{it} denote the number of adult consumers residing in location $i \in \mathcal{N}$ at time t, and let the vector $\mathbf{L}_t \equiv (L_{1t}, L_{2t}, \ldots, L_{Nt})^\top \in \mathbb{R}^N_{\geq 0}$ represent the *population distribution*. The set of all feasible population distributions at each period is denoted by $\mathcal{L} \equiv \{\mathbf{L}_t \in \mathbb{R}^N_{\geq 0} \mid \sum_{i \in \mathcal{N}} L_{it} = L\}$. Commuting across locations is not allowed, so that all agents supply labor in the same location where they reside.

Each location $i \in \mathcal{N}$ produces a unique variety of a differentiated good as in Armington (1969). Production is perfectly competitive, and each firm at location i uses only labor, supplied inelastically by local residents, as an input. Goods trade between locations is subject to iceberg transport costs.

As will be specified later, the AD model assumes that externalities arise depending on local population sizes. Let A_i denote the productivity and u_i the amenity level of location i. Both are assumed to depend on the number of residents at that location, potentially increasing or decreasing with population.

Firms. At each location $i \in \mathcal{N}$, firms produce and supply goods under perfect competition. Labor is the sole input. Under the assumption, the factory-gate price p_i of the good produced at location i equals its marginal cost: $p_i = w_i / A_i$. Here, A_i denotes the aggregate marginal productivity of labor at location i.

To capture inter-generational externalities, A_i depends on t, and $A_i = A_{it}$ is assumed to depend on the number of workers at location i in the current and previous periods:

$$A_{it}(L_{it}, L_{i,t-1}) = \bar{A}_i L_{it}^{\alpha_1} L_{i,t-1}^{\alpha_2} \tag{A}$$

where $\bar{A}_i > 0$, $\alpha_1 \geq 0$, and $\alpha_2 > 0$ are given constants.

The parameter α_1 captures the strength of the positive externality arising from *current* population agglomeration: the greater the local concentration of workers, the higher the productivity of labor at that location. The parameter α_2 represents the strength of the externality due to *past* agglomeration, implying that higher population in the previous period raises current productivity. Finally, $\bar{A}_i$ is the innate productivity coefficient of region i.

Consumers/Workers. Only adult agents engage in consumption. The utility of

a consumer residing in location $i \in \mathcal{N}$ is given by

$$W_i = u_i(L_i)\Big(\sum_{j\in\mathcal{N}} q_{ji}^{\frac{\sigma-1}{\sigma}}\Big)^{\frac{\sigma}{\sigma-1}}. \tag{1}$$

Here, q_{ji} denotes the quantity consumed of the good variety produced in location $j \in \mathcal{N}$, and $\sigma > 1$ is the elasticity of substitution across varieties. Let p_{ji} denote the price at which the variety produced in j is sold to consumers in i, and let $w_i \geq 0$ denote the wage income of a consumer in location i. Maximizing utility subject to the budget constraint $w_i = \sum_{j\in\mathcal{N}} p_{ji}q_{ji}$ yields the following demand for each variety:

$$q_{ji} = \frac{p_{ji}^{-\sigma}}{P_i^{1-\sigma}}w_i, \quad \text{where} \quad P_i = \left(\sum_{k\in\mathcal{N}} p_{ki}^{1-\sigma}\right)^{\frac{1}{1-\sigma}}. \tag{2}$$

Given a nonzero price vector $\boldsymbol{p} \neq \mathbf{0}$ and wage rate vector $\boldsymbol{w}$, the indirect utility of a consumer residing in location i is:

$$W_{it} = u_{it}w_{it}P_{it}^{-1}, \tag{3}$$

where u_{it} represents the amenity level in location i at time t.

To incorporate externalities, we assume that the amenity level u_{it} at location i and time t depends on the number of workers currently and previously residing there, L_{it} and $L_{i,t-1}$:

$$u_{it}(L_{it}, L_{i,t-1}) = \bar{u}_i L_{it}^{\beta_1} L_{i,t-1}^{\beta_2} \tag{u}$$

where $\bar{u}_i > 0$, $\beta_1 < 0$, and $\beta_2 > 0$ are fixed parameters.

The signs of β_1 and β_2 differ. The parameter β_1 captures negative *current* externalities (e.g., traffic congestion or increased land prices) that degrade living conditions as population density rises. In contrast, β_2 reflects positive externalities stemming from *past* agglomeration, such as infrastructure accumulation or urban amenities, and is assumed to be strictly positive.

Goods trade. Delivering one unit of a good from location i to location j requires shipping $\tau_{ij} > 1$ units from i to $j \neq i$ and $\tau_{ii} = 1$ for all i. The price at which the variety produced in i is sold to consumers in j is $p_{ij} = p_i\tau_{ij}$. In turn, the value of

trade from location i to location j, denoted X_{ij}, is

$$X_{ij} = \tau_{ij}^{1-\sigma} \left(\frac{w_i}{A_i} \right)^{1-\sigma} P_j^{\sigma-1} w_j L_j, . \tag{4}$$

From the setup so far, this price index can be expressed as:

$$P_j = \left(\sum_{k \in \mathcal{N}} \left(\frac{w_k}{A_k} \right)^{1-\sigma} d_{kj} \right)^{1/(1-\sigma)}, \tag{5}$$

where $d_{kj} \equiv \tau_{kj}^{1-\sigma} \in (0, 1]$.

Location Choice. Working-age consumers are assumed to choose their residential location. The utility from migrating from location i to location j using a migration resistance parameter μ_{ij}. That is, $W_{ij} \equiv \epsilon_{ij} W_j / \mu_{ij}$, where ϵ_{ij} captures idiosyncratic preferences that are not explained by the deterministic component of the model (W_j). Consumers choose their location in the next period by maximizing this idiosyncratic utility.

The idiosyncratic component ϵ_{ij} follows an i.i.d. Fréchet distribution with shape parameter $\theta > 0$. Under this assumption, the probability that an individual in location i chooses to move to location j is given by:

$$S_{ijt} = \frac{\left(W_{jt} / \mu_{ij} \right)^{\theta}}{\sum_{k \in \mathcal{N}} \left(W_{kt} / \mu_{ik} \right)^{\theta}}. \tag{6}$$

The parameter θ reflects the degree of preference homogeneity across individuals. As $\theta \to 0$, location choice becomes entirely random and insensitive to W, representing maximum heterogeneity. As $\theta \to \infty$, agents become homogeneous and choose the location with the highest deterministic utility.[1]

The number of migrants from location i to location j is then:

$$L_{ijt} = S_{ijt} L_{i,t-1} = \frac{\left(W_{jt} / \mu_{ij} \right)^{\theta}}{\sum_{k \in \mathcal{N}} \left(W_{kt} / \mu_{ik} \right)^{\theta}} L_{i,t-1}. \tag{7}$$

Intertemporal equilibrium. The equilibrium conditions consist of the following, where we make the time index explicit:

- **Zero-profit condition for firms.** At each location i, the total revenue of firms equals the total wage payments to consumers residing there: $w_{it} L_{it} =$

[1] Such randomness is isomorphically represented as the consumption of nontraded goods (Behrens and Murata, 2021).

$\sum_j X_{ijt}$. Substituting from Eq. (4), we obtain:

$$w_{it}^{\sigma} L_{it}^{1-\alpha_1(\sigma-1)} = \sum_j K_{ijt} L_{jt}^{\beta_1(\sigma-1)} W_{jt}^{1-\sigma} w_{jt}^{\sigma} L_{jt} \tag{8}$$

- **Goods market clearing.** Consumers spend all of their income on consumption: $w_{it} L_{it} = \sum_j X_{jit}$. From Eq. (4), this gives:

$$w_{it}^{1-\sigma} L_{it}^{\beta_1(1-\sigma)} W_{it}^{\sigma-1} = \sum_j K_{jit} L_{jt}^{\alpha_1(\sigma-1)} w_{jt}^{1-\sigma}, \tag{9}$$

$$\text{where} \quad K_{ijt} \equiv \left(\frac{\tau_{ij}}{\bar{A}_{it} L_{i,t-1}^{\alpha_2} \bar{u}_{jt} L_{j,t-1}^{\beta_2}} \right)^{1-\sigma}. \tag{10}$$

  These two equations jointly express that the total flow of payments across the economy is conserved.

- **Migration equilibrium.** The population at location i in period t equals the sum of incoming migrants from all other locations: $L_{it} = \sum_j L_{jit}$. Using Eq. (7), this can be written as:

$$L_{it} W_{it}^{-\theta} = \sum_j \mu_{jit}^{-\theta} \Pi_{jt}^{-\theta} L_{jt-1}, \tag{11}$$

  where $\Pi_{it} \equiv \mathbb{E}\left[\max_j W_{ijt}\right] = \left(\sum_k (W_{kt}/\mu_{ikt})^{\theta}\right)^{1/\theta}$.

3 Analysis

3.1 Steady-state equilibrium and its stability

The dynamics of the population distribution $\mathbf{L}$ are governed by the market and migration equilibrium conditions Eqs. (8) to (11). Specifically, given the population distribution in the previous period $\mathbf{L}_{t-1}$, one can solve the current-period market and migration equilibrium conditions simultaneously to obtain $\mathbf{L}_t$. This defines a discrete-time dynamical system of the form $\mathbf{L}_{t-1} \mapsto \mathbf{L}_t$.

Let $\mathbf{F}(\cdot)$ denote the operator that maps $\mathbf{L}_{t-1}$ to $\mathbf{L}_t$ through the equilibrium conditions. Then the system can be written as:

$$\mathbf{L}_t = \mathbf{F}(\mathbf{L}_{t-1}). \tag{12}$$

The operator $\mathbf{F}$ is implicitly defined by the following equilibrium conditions that summarizes Eqs. (8) to (11):

$$z_{1i}(\boldsymbol{w}_t, \mathbf{L}_t, \mathbf{L}_{t-1}) = w_{it}L_{it} - \sum_{k\in\mathcal{N}} M_{ikt}w_{kt}L_{kt} = 0, \tag{13}$$

$$z_{2i}(\boldsymbol{w}_t, \mathbf{L}_t, \mathbf{L}_{t-1}) = L_{it} - \sum_{k\in\mathcal{N}} S_{ikt}L_{kt-1} = 0, \tag{14}$$

where

$$M_{ijt} \equiv \frac{K_{ikt}L_{it}^{\alpha_1(\sigma-1)}w_{it}^{1-\sigma}}{\sum_{l\in\mathcal{N}} K_{lkt}L_{lt}^{\alpha_1(\sigma-1)}w_{lt}^{1-\sigma}}, \quad S_{ijt} \equiv \frac{\mu_{ikt}^{-\theta}W_{it}^{\theta}}{\sum_{l\in\mathcal{N}} \mu_{lkt}^{-\theta}W_{lt}^{\theta}}, \tag{15}$$

and K_{ijt} is defined by Eq. (10).

We are particularly interested in steady-state equilibria that satisfy

$$\mathbf{L}^* = \mathbf{F}(\mathbf{L}^*), \tag{16}$$

and in analyzing their stability under the discrete-time dynamic (12).

Local stability of such an equilibrium can be determined by the eigenvalues $\{f_k\}$ of the Jacobian matrix $\nabla\mathbf{F}(\mathbf{L}^*)$. Specifically, if every eigenvalue satisfies $\max\{|f_k|\} < 1$, then the steady-state is locally stable. Otherwise, it is unstable. To see this, consider a small perturbation $\boldsymbol{\epsilon}_{t-1}$ around the fixed point such that $\tilde{\mathbf{L}}_{t-1} \equiv \mathbf{L}^* + \boldsymbol{\epsilon}_{t-1}$. The subsequent evolution of the state is then given by

$$\tilde{\mathbf{L}}_t = \mathbf{F}(\tilde{\mathbf{L}}_{t-1}) \approx \mathbf{F}(\mathbf{L}^*) + \nabla\mathbf{F}(\mathbf{L}^*)\boldsymbol{\epsilon}_{t-1} = \mathbf{L}^* + \nabla\mathbf{F}(\mathbf{L}^*)\boldsymbol{\epsilon}_{t-1}. \tag{17}$$

Because $\boldsymbol{\epsilon}_t = \tilde{\mathbf{L}}_t - \mathbf{L}^*$, in a neighborhood of the fixed point $\mathbf{L}^*$, the dynamics of the perturbation follow:

$$\boldsymbol{\epsilon}_t = \nabla\mathbf{F}(\mathbf{L}^*)\boldsymbol{\epsilon}_{t-1}. \tag{18}$$

If $\boldsymbol{\epsilon}_t \to \mathbf{0}$ as $t \to \infty$ for any sufficiently small initial perturbation, then the fixed point $\mathbf{L}^*$ is stable. This occurs if and only if all eigenvalues of $\nabla\mathbf{F}(\mathbf{L}^*)$ have modulus strictly less than 1.

The Jacobian matrix $\nabla\mathbf{F}(\mathbf{L})$ can be analytically obtained by totally differentiation of the equilibrium system described above, as shown in Appendix A.

Each eigenvector $\boldsymbol{\epsilon}$ of $\nabla\mathbf{F}(\mathbf{L}^*)$ satisfying $\sum_{i\in\mathcal{N}} \epsilon_i = 0$ corresponds to a feasible migration pattern, and the associated eigenvalue represents the amplification factor of that migration pattern from period $t-1$ to t.

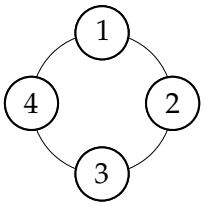

Figure 5: The four-region circular economy.

Compared to continuous-time adjustment dynamics as considered in static spatial models for equilibrium refinement, a key distinction in this discrete-time setting is that the *sign* of the eigenvalue also carries important meaning. Even when the modulus is less than one (implying decay), a negative eigenvalue implies that the associated perturbation oscillates in sign over time.

For instance, in a symmetric two-location model, a small perturbation around the symmetric equilibrium $\bar{\mathbf{L}} \equiv (L/2, L/2)$ can be written as $\bar{\mathbf{L}} + \epsilon \times (1, -1) = (L/2 + \epsilon, L/2 - \epsilon)$, where $(1, -1)$ is an eigenvector. If the eigenvalue is f, in the next period, it evolves into $(L/2 + f\epsilon, L/2 - f\epsilon)$. If $f < 0$, the ranking of population sizes between the two regions alternates over time, that is, oscillation occurs. Whether such oscillatory dynamics occur in practice is an interesting empirical question, but from the standpoint of quantitative policy analysis, the emergence of oscillations may pose interpretative or computational challenges.

To assess local stability of a stationary equilibrium $\mathbf{L}^*$, one must derive the eigensystem of $\nabla \mathbf{F}(\mathbf{L}^*)$ at the steady-state equilibrium $\mathbf{L}^*$. In general, however, analytical characterization of $\mathbf{L}^*$ is infeasible under asymmetric geographies. In the following analysis, we focus on symmetric spatial settings to focus on the role of endogenous forces in the AD model.

3.2 Four-location circular economy

Below, we assume a circular four-location geography. This system provides a minimal yet sufficient setting to investigate the essential features of spatial models of agglomeration. As Matsuyama (2017) puts it, "it is the smallest number in which a different region can have different neighbors, even though they are all symmetrically located." Notably, three is not enough. The circular four-location system is particularly suitable for identifying whether the model admits multiple stable equilibria, and if so, whether such equilibria exhibit a multi-core spatial pattern (in which multiple large cities emerge) or a monocentric pattern (in which a single dominant mega-region forms).

Figure 5 illustrates the four-location circe. All locations are placed equidis-

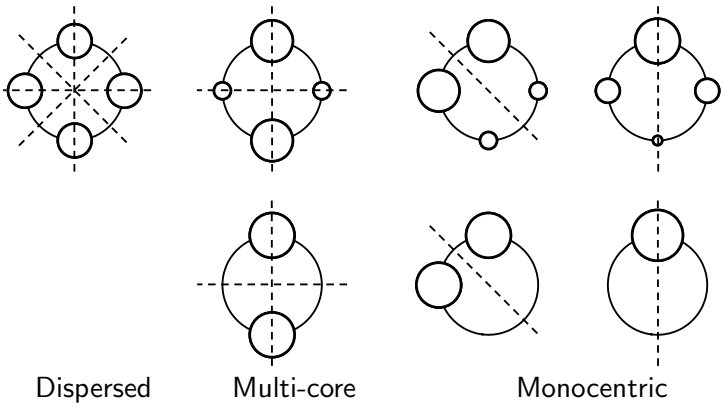

Figure 6: Schematic diagram of all possible equilibrium patterns in a symmetric circular economy with four locations.

tantly on the unit circle. In the AD model, assuming spatially uniform innate amenity levels $\bar{A}_i$ and productivity levels $\bar{u}_i$, the only source of heterogeneity across locations lies in their relative positions on the transportation network. In the circular four-location system, all locations are symmetric in this spatial sense as well.

In this setting, the *dispersed pattern* in which consumers are evenly distributed across all locations, $\bar{\mathbf{L}} = [l, l, l, l]^\top$ with $l = L/4$, is a trivial equilibrium solution.

Figure 6 presents schematic illustrations of all possible equilibrium configurations in the symmetric four-location circular system (see, e.g., Ikeda et al., 2012). The size of the circles in the diagram represents the relative population size at each location. Each illustrated equilibrium exhibits mirror symmetry with respect to a dashed axis.

The distance between two locations in the circular system is defined as the shortest arc length along the circle, and is given by:

$$t_{ij} = \min\left\{|i-j|, 4-|j-i|\right\}. \tag{19}$$

The iceberg trade cost parameter τ_{ij} between locations i and j is assumed to take the form $\tau_{ij} = \tau^{t_{ij}}$, where $\tau > 1$ is a global iceberg cost parameter. The closer τ is to 1, the more frictionless is trade across locations.

Migration resistance μ_{ij} is similarly assumed to be distance-dependent, with $\mu_{ij} = \mu^{t_{ij}}$ for some global parameter $\mu > 1$. As with trade, the closer μ is to 1, the more freely agents can move between locations.

Under these assumptions, we define two *spatial discount matrices*, $\mathbf{D} = [d_{ij}]$ and $\mathbf{E} = [e_{ij}]$, where the (i,j)-th entries are given by $d_{ij} = \tau_{ij}^{1-\sigma} = \tau^{(1-\sigma)t_{ij}}$ and

$e_{ij} = \mu_{ij}^{-\theta} = \mu^{-\theta t_{ij}}$, respectively. The matrix $\mathbf{D}$ captures the trade frictions between regions, while $\mathbf{E}$ represents the resistance to migration across regions.

For analytical convenience, we define the *trade freeness* $r \in (0,1)$ and the *migration freeness* $s \in (0,1)$ as follows:

$$r = \tau^{(1-\sigma)}, \quad s = \mu^{-\theta}. \tag{20}$$

Using these definitions, the matrices $\mathbf{D}$ and $\mathbf{E}$ can be simply rewritten as:

$$\mathbf{D} = \begin{bmatrix} 1 & r & r^2 & r \\ r & 1 & r & r^2 \\ r^2 & r & 1 & r \\ r & r^2 & r & 1 \end{bmatrix}, \quad \mathbf{E} = \begin{bmatrix} 1 & s & s^2 & s \\ s & 1 & s & s^2 \\ s^2 & s & 1 & s \\ s & s^2 & s & 1 \end{bmatrix}. \tag{21}$$

As r approaches 1, the global trade cost τ becomes close to 1, corresponding to a nearly frictionless goods market across locations. Likewise, s approaching 1 implies a low migration resistance, i.e., a highly mobile population. In the analysis that follows, we examine how changes in the economy-wide trade and migration costs (equivalently, in the parameters r and s) affect the spatial agglomeration patterns that emerge in equilibrium.

3.3 Stability of the dispersed equilibrium

We now consider the conditions under which the dispersed equilibrium $\bar{\mathbf{L}} = [l, l, l, l]$ ($l = L/4$) is stable. We investigate how the population distribution evolves under the AD model as the degrees of trade freeness r and migration freeness s vary. As discussed in Section 2, the stability of the dispersed equilibrium $\bar{\mathbf{L}}$ can be determined by analyzing the eigenvalues $\boldsymbol{f}$ of the Jacobian matrix $\nabla\mathbf{F}(\bar{\mathbf{L}})$ that governs the inter-temporal dynamics.

Due to the special structure of the spatial discount matrices $\mathbf{D}$ and $\mathbf{E}$, the eigenvalue analysis of $\nabla\mathbf{F}(\mathbf{L})$ becomes tractable. Specifically, the eigenvalues of $\nabla\mathbf{F}(\bar{\mathbf{L}})$ can be expressed in terms of those of the spatial discount matrices. To this end, define

$$T_k(x) \equiv \begin{cases} 1 & \text{if } k = 0 \\ C(x) & \text{if } k = 1, 3 \\ C(x)^2 & \text{if } k = 2 \end{cases} \quad \text{with} \quad C(x) \equiv \frac{1-x}{1+x}. \tag{22}$$

Then, the eigenvalues of $\mathbf{D}$ and $\mathbf{E}$ are cleanly obtained as follows:

Lemma 1. *Let χ_k and λ_k denote the k-th eigenvalues ($k = 0, 1, 2, 3$) of the normalized spatial discount matrices $\bar{\mathbf{D}} \equiv (1+r)^{-2}\mathbf{D}$ and $\bar{\mathbf{E}} \equiv (1+s)^{-2}\mathbf{E}$, respectively, in the circular four-location system. Then, $\chi_k = T(r)$ and $\lambda_k = T(s)$. For $k \neq 0$, both χ_k and λ_k are strictly decreasing functions of $r \in (0,1)$ and $s \in (0,1)$, respectively. Moreover,*

$$0 < \chi_2 < \chi_1 = \chi_3 < \chi_0 = 1 \quad \textit{and} \quad 0 < \lambda_2 < \lambda_1 = \lambda_3 < \lambda_0 = 1 \tag{23}$$

for any fixed (r, s). The corresponding (normalized) eigenvectors are:

$$\boldsymbol{\epsilon}_k \equiv \begin{cases} \langle 1,1,1,1 \rangle & \textit{if } k = 0 \\ \langle 1,0,-1,0 \rangle \textit{ or } \langle 1,1,0,0 \rangle & \textit{if } k = 1,3 \\ \langle 1,-1,1,-1 \rangle & \textit{if } k = 2 \end{cases} \tag{24}$$

Here, for a vector $\boldsymbol{v}$, $\langle \boldsymbol{v} \rangle$ denotes the normalized vector $\boldsymbol{v}/\|\boldsymbol{v}\|$.

The eigenvector corresponding to $k = 0$, $\langle 1,1,1,1 \rangle$, represents perturbations in which the population increases uniformly across all regions. Since the total population is fixed, this direction is irrelevant to the stability analysis.

The eigenvectors corresponding to $k = 1$ (and $k = 3$) represent migration patterns associated with the formation of a *monocentric* distribution, as illustrated in Fig. 2B. On the other hand, $k = 2$ corresponds to a *polycentric* (more specifically, duo-centric) distribution. We henceforth focus on $k = 1, 2$.

Using the eigenvalues $\{\chi_k\}$ and $\{\lambda_k\}$, we can explicitly express the eigenvalues (i.e., the growth rates of perturbations) of $\nabla\mathbf{F}(\bar{\mathbf{L}})$ along the monocentric ($k = 1$) and polycentric ($k = 2$) directions.

Lemma 2. *The k-th eigenvalue f_k of $\nabla\mathbf{F}(\bar{\mathbf{L}})$ is given by $f_k = \frac{h_k^\sharp}{h_k^\flat}$, where:*

$$h_k^\sharp = \alpha_2 A_k + \beta_2 + \frac{\lambda_k}{\theta(1-\lambda_k^2)}, \tag{25}$$

$$h_k^\flat = -\alpha_1 A_k - \beta_1 + B_k + \frac{1}{\theta(1-\lambda_k^2)}, \tag{26}$$

$$A_k = \frac{\chi_k + (\sigma-1)(1+\chi_k)}{1+(\sigma-1)(1+\chi_k)} \in (0,1), \quad B_k = \frac{1-\chi_k}{1+(\sigma-1)(1+\chi_k)} > 0. \tag{27}$$

The eigenvector corresponding to f_k is given in Eq. (24).

Proof. See Appendix A. □

Note that the terms involving λ_k represent mechanisms related to migration frictions while those involving χ_k correspond to trade frictions. If all externalities

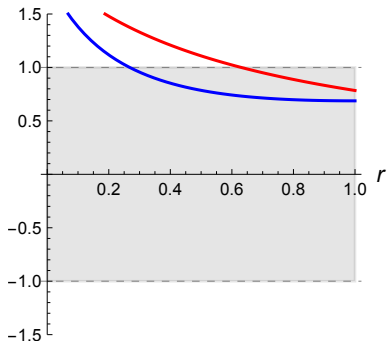

Figure 7: Typical shape of eigenvalue functions f.

Note: Red: monocentric direction (f_1). Blue: polycentric direction (f_2). The dispersed equilibrium is unstable if either of the curves are outside the gray region. We set $(\alpha_1, \beta_1, \alpha_2, \beta_2, \sigma, \theta) = (0.7, -0.4, 0, 0, 8, 6)$ and $s = 0.5$.

are turned off ($\alpha_1 = \alpha_2 = \beta_1 = \beta_2 = 0$), we have

$$f_k = \frac{\lambda_k}{\theta(1-\lambda_k^2)B_k + 1} \in (0,1).$$

because $\lambda_k \in (0,1)$ and $B_k > 0$. This shows that the dispersed equilibrium $\bar{\mathbf{L}}$ is stable for all admissible (r,s). That is, in the absence of externalities, endogenous agglomeration due to instability cannot arise.

3.4 Agglomeration from the dispersed equilibrium

If there are externalities, the dispersed equilibrium can become unstable, and endogenous agglomeration can occur. In this section, we use the eigenvalues $\{f_k\}$ derived in the previous section to characterize the agglomeration properties of the AD model. As discussed earlier, agglomeration from the dispersed state occurs when the absolute value of an eigenvalue f_k ($k = 1, 2$) crosses the unit threshold: that is, when $|f_k|$ exceeds 1. In particular, if $|f_1|$ exceeds 1 first, agglomeration proceeds in the *monocentric direction*; if $|f_2|$ does, agglomeration occurs in the *polycentric direction*.

First, note that under $\sigma > 1$, $0 < \chi < 1$, and $0 < \lambda < 1$, we have $A_k > 0$ and $B_k > 0$, which implies that $h_k^\sharp > 0$ for all parameter values. Meanwhile, the negative terms in $h_k^\flat$ all involve α_1. Therefore, regarding the sign of f_k, we obtain the following observation:

- If $\alpha_1 = 0$, then $f_k > 0$.
- If $\alpha_1 \neq 0$, then $f_k < 0$ can occur for certain combinations of (α_1, β_1) that lead to $h_k^\flat < 0$.

In regions where $f_k < 0$, the system exhibits *oscillatory dynamics*, leading either to agglomeration or reversion to dispersion through non-monotonic paths. It is recalled that the parameter α_1 reflects the strength of contemporaneous agglomeration effects: its influence is independent of past agglomeration. Hence, when α_1 is sufficiently large relative to β_1, oscillatory behavior may arise—an outcome that is arguably less realistic in empirical settings, as population agglomeration usually proceeds monotonically over time.

Next, observe the following comparative statics: since A_k increases and B_k decreases with respect to χ_k, we deduce that f_k is monotonically increasing in χ_k and hence monotonically decreasing in r. Indeed,

$$\frac{\partial h_k^\sharp}{\partial \chi_k} = \alpha_2 \frac{\partial A_k}{\partial \chi_k}, \qquad \frac{\partial h_k^\flat}{\partial \chi_k} = -\alpha_1 \frac{\partial A_k}{\partial \chi_k} + \frac{\partial B_k}{\partial \chi_k}. \tag{28}$$

Since $\frac{\partial h_k^\sharp}{\partial \chi_k} > 0$ and $\frac{\partial h_k^\flat}{\partial \chi_k} < 0$, and assuming $h_k^\flat > 0$, it follows that

$$\frac{\partial f_k}{\partial \chi_k} = \frac{1}{h_k^\flat} \frac{\partial h_k^\sharp}{\partial \chi_k} - \frac{h_k^\sharp}{(h_k^\flat)^2} \frac{\partial h_k^\flat}{\partial \chi_k} > 0. \tag{29}$$

Based on this result, we establish the following proposition regarding the effect of trade freeness r on agglomeration patterns.

Proposition 1. *Suppose that for some k, $|f_k|$ exceeds 1 as a result of changes in r.*

(a) If $f_k < 0$, increasing r induces agglomeration in the polycentric (duo-centric) direction.

(b) If $f_k > 0$, decreasing r induces agglomeration in the monocentric direction.

Proof. From Lemma 1, we have $\chi_2 < \chi_1$. As r increases (i.e., χ decreases), the first instability arises in f_2, whose eigenvector is $\boldsymbol{z}_2 = \langle 1, -1, 1, -1 \rangle$, corresponding to the polycentric direction. Conversely, as r decreases (i.e., χ increases), the first instability arises in f_1, with eigenvectors $\langle 1, 0, -1, 0 \rangle$ or $\langle 1, 1, 0, 0 \rangle$, corresponding to the monocentric direction. For illustration, Figure 7 shows typical eigenvalue trajectories $f_k(r)$, including those with negative values. □

This result implies the following: if the dispersed equilibrium loses stability and agglomeration proceeds *monotonically* (i.e., without oscillations), then the agglomeration must occur in the *monocentric direction*. This finding is similar to the static AA model as discussed in Akamatsu et al. (2017, 2024). This is natural because the AD framework is its dynamic extension.

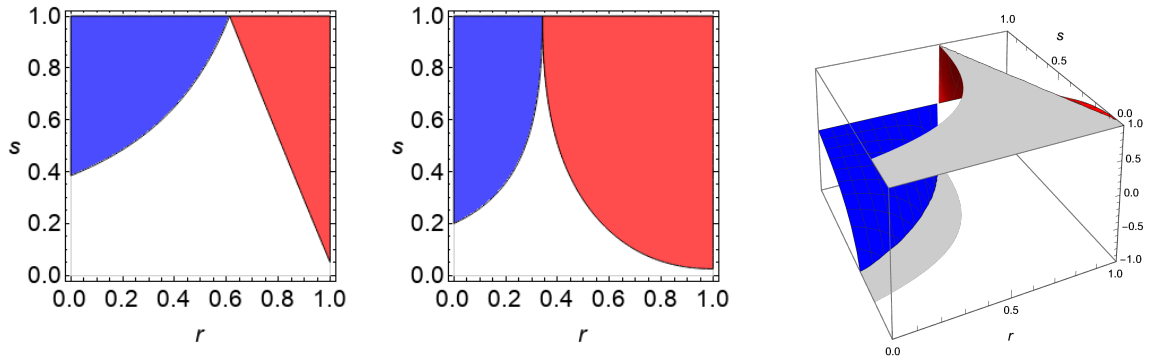

(A) $-1 < f_1 < 1$ (B) $-1 < f_2 < 1$ (C) Shape of f_1

Figure 8: Regions where the modulus of f_1 and f_2 are less than 1

Note: We set $(\alpha_1, \beta_1, \alpha_2, \beta_2, \sigma, \theta) = (0.7, -0.4, 0, 0, 8, 6)$.

4 Numerical Examples

Numerical examples illustrate how each model parameter influences the behavior of the system.

4.1 Stability Region of the Dispersed Equilibrium

Figures 8A and 8B illustrate the regions in which the modulus of the eigenvalues f_1 and f_2 remain below 1. The horizontal axis represents the degree of trade freeness r, and the vertical axis represents the degree of migration freeness s. In each panel, the red region corresponds to $0 < f_k < 1$, and the blue region to $-1 < f_k < 0$. Each eigenvalue tends to become negative in regions where trade freeness is low and migration freeness is high.

The parametric regions where eigenvalues are negative correspond to cases where the dispersed equilibrium becomes unstable and oscillatory dynamics emerge. Figure 9 overlays the two subfigures from Fig. 8. The dispersed equilibrium $\bar{\mathbf{L}}$ is stable in the regions labeled (a), (b), and (c), where the two individual stability regions intersect.

For (r, s) such that satisfy both $f_1 \in (-1, 1)$ and $f_2 \in (-1, 1)$, the dispersed equilibrium remains stable. If (r, s) slowly vary and we cut the boundary of this region, instability occurs and nontrivial spatial patterns emerges.

As shown in Fig. 9, the ways in which the dispersed equilibrium $\bar{\mathbf{L}}$ loses stability are diverse. The possible directions in which instability arises are indicated by black arrows in the figure.

Region (c) (the red region). Instability of $\bar{\mathbf{L}}$ occurs when both r and s decrease.

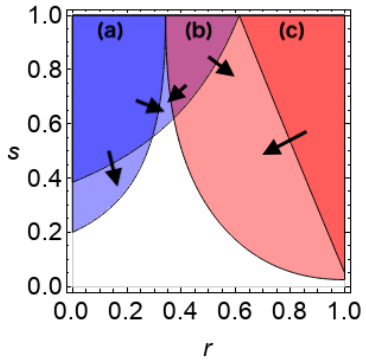

Figure 9: Stability region

In this case, instability arises as f_1 exceeds 1. This leads to a non-oscillatory shift in the population distribution toward a monocentric pattern.

Region (b) (the purple region). Instability of $\bar{\mathbf{L}}$ occurs in two ways:

- If instability occurs as r increases, it is due to f_1 becomes smaller than -1. In this case, the population distribution still follows the monocentric direction but exhibits oscillatory dynamics. That is, if region 1 initially becomes dominant, it is subsequently replaced by region 3, and so on in alternation.
- If instability occurs as r decreases, it results from f_2 exceeding 1. This leads to a monotonic transition toward a polycentric pattern, for example, a gradual concentration in regions 1 and 3. However, this case only arises in a narrow region of the parameter space.

It should be noted that region (b) is surrounded by unstable regions, implying that this region may be less relevant.

Region (a) (the blue region). Instability of $\bar{\mathbf{L}}$ occurs occurs in two ways:

- If instability arises in the upper part of the region (i.e., for high s), it is due to f_2 going below -1. In this case, the population distribution moves in the polycentric direction, but in an oscillatory fashion. For instance, if regions 1 and 3 initially become dominant, they are later replaced by regions 2 and 4, and so on in alternation.
- If instability occurs in the lower part (i.e., for low s), it results from f_1 going below -1, leading to oscillatory dynamics in the monocentric direction.

In summary, if agglomeration should occur without oscillation, it generally occurs only in the monocentric direction. Although stable transitions in the poly-

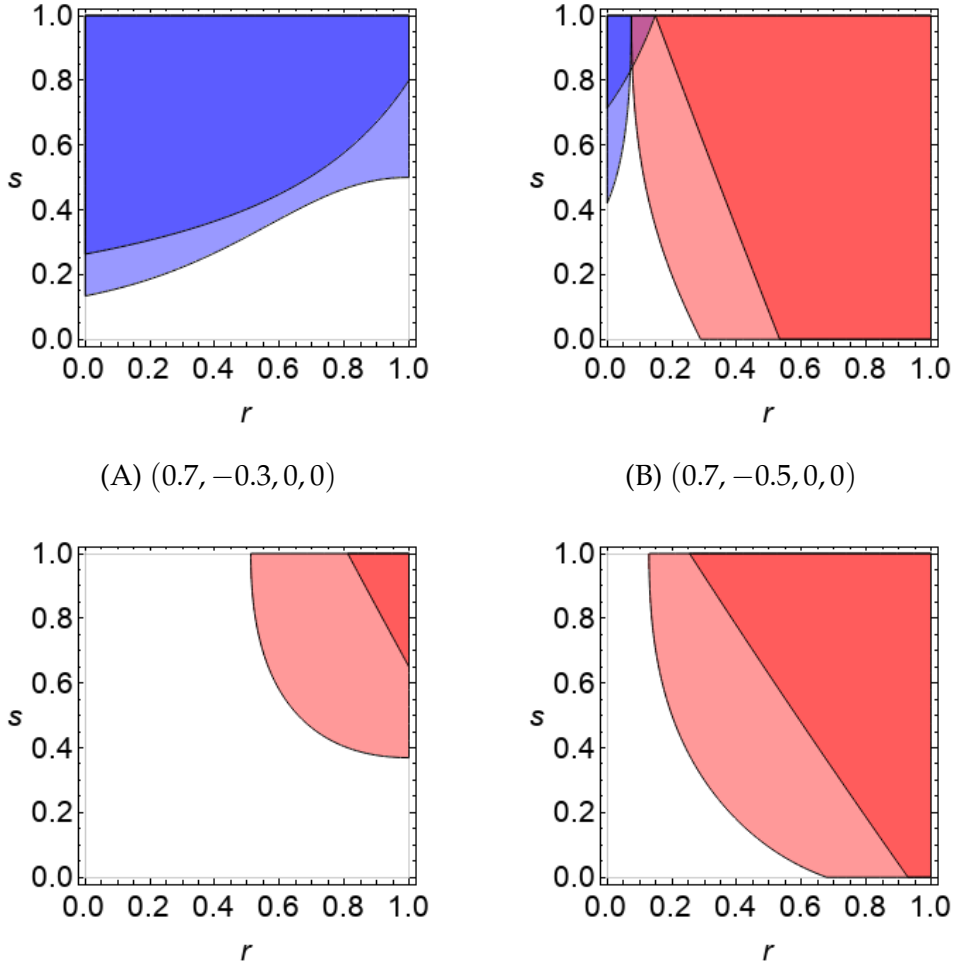

(A) $(0.7, -0.3, 0, 0)$ (B) $(0.7, -0.5, 0, 0)$

(C) $(0, 0, 0.3, 0)$ (D) $(0, 0, 0, 0.2)$

Figure 10: Effects of varying $(\alpha_1, \beta_1, \alpha_2, \beta_2)$ with $(\sigma, \theta) = (8, 6)$

centric direction are theoretically possible, they arise only in a narrowly confined region.

4.2 Changes in Stability due to Parameter Variations

This subsection examines how changes in the model parameters affect the stability region. Figures 10A and 10B show results for fixed $\alpha_1 = 0.7$, with β_1 varied between -0.3 and -0.5.

The parameter α_1 captures the strength of contemporaneous agglomeration. That is, the force generating new agglomeration regardless of past distributions. As α_1 increases relative to β_1, the region in which the eigenvalues are negative expands. Moreover, even in regions where eigenvalues are positive, an increase in α_1 contributes to instability by amplifying the negative terms in the denomi-

nator of the eigenvalue expressions.

In contrast, β_1 represents the strength of contemporaneous dispersion. Increasing β_1 enlarges the region in which the eigenvalues are positive, and thereby expands the overall stability region. Decreasing β_1 relative to α_1 enlarges the region where eigenvalues are negative. As seen in Fig. 9, appropriate settings of α_1 and β_1 can produce multiple stable regions, with instability arising from both increases and decreases in trade costs.

The parameters α_2 and β_2 measure the effects of agglomeration at the previous period $t-1$ on current location utility. In other words, they increase persistence, or the inertia of spatial agglomeration from the previous period. Accordingly, as shown in Figs. 10C and 10D, the system tends to exhibit only monocentric agglomeration (corresponding to region (a) in Fig. 9).

5 Concluding remarks

This paper has explored the agglomeration properties of the AD model, a dynamic spatial framework that incorporates inter-generational agglomeration externalities and endogenous migration. With the properties of its static counterpart (the AA model) in mind, we examined whether similar structural features persist once dynamic feedback and migration are introduced. Using a stylized environment, we showed that the AD model also yields stable equilibrium trajectories only in the form of single-core agglomeration, provided inter-temporal oscillations are excluded. In this sense, the dynamic framework largely inherits the qualitative behavior of its static version, including the monotonic tendency toward spatial dispersion as transport costs fall.

The analysis presented here is deliberately based on a simplified setting, designed to isolate the model's core mechanisms. While the original AD study considers richer environments (asymmetric geographies) for quantitative applications, our focus has been on clarifying the theoretical behavior of the model in a transparent setting.

Our results suggest that the AD model can, in principle, generate polycentric outcomes through oscillatory dynamics. However, the empirical relevance of such fluctuations remains uncertain. In applied contexts where stability and tractability are essential, this may limit the model's effectiveness in capturing the multi-centered spatial patterns observed in real-world economies.

Nonetheless, the AD framework represents an important step toward bridging static and dynamic approaches to spatial analysis. It offers a coherent frame-

work for studying how localized externalities accumulate over time and influence interregional outcomes. Our contribution complements this broader research agenda by highlighting the specific conditions under which the dynamic model replicates, or departs from, the qualitative properties of its static counterpart.

Developing dynamic models that flexibly accommodate both single-core and polycentric agglomeration under empirically plausible conditions remains a promising direction for future research, particularly in economies undergoing rapid structural transformation and declining transport costs.

A Derivations

We recall that the equilibrium conditions can be summarized as follows:

$$z_{1i}(\boldsymbol{w}_t, \mathbf{L}_t, \mathbf{L}_{t-1}) = w_{it}L_{it} - \sum_{k\in\mathcal{N}} \frac{K_{ikt}L_{it}^{\alpha_1(\sigma-1)}w_{it}^{1-\sigma}}{\sum_{l\in\mathcal{N}} K_{lkt}L_{lt}^{\alpha_1(\sigma-1)}w_{lt}^{1-\sigma}} w_{kt}L_{kt} \tag{30}$$

$$= w_{it}L_{it} - \sum_{k\in\mathcal{N}} m_{ikt}w_{kt}L_{kt}, \tag{31}$$

$$z_{2i}(\boldsymbol{w}_t, \mathbf{L}_t, \mathbf{L}_{t-1}) = L_{it} - \sum_{k\in\mathcal{N}} \frac{\mu_{ikt}^{-\theta}W_{it}^{\theta}}{\sum_{l\in\mathcal{N}} \mu_{lkt}^{-\theta}W_{lt}^{\theta}} L_{kt-1} \tag{32}$$

$$= L_{it} - \sum_{k\in\mathcal{N}} S_{ikt}L_{kt-1}. \tag{33}$$

That is,

$$\boldsymbol{z}(\boldsymbol{w}_t, \mathbf{L}_t, \mathbf{L}_{t-1}) \equiv \begin{bmatrix} \boldsymbol{z}_1(\boldsymbol{w}_t, \mathbf{L}_t, \mathbf{L}_{t-1}) \\ \boldsymbol{z}_2(\boldsymbol{w}_t, \mathbf{L}_t, \mathbf{L}_{t-1}) \end{bmatrix} = \begin{bmatrix} (\mathbf{I} - \mathbf{M}_t)(\mathbf{Y}_t) \\ \mathbf{L}_t - \mathbf{S}_t\mathbf{L}_{t-1} \end{bmatrix} = \mathbf{0}, \tag{34}$$

where $Y_{it} = w_{it}L_{it}$. The (i,j)th element of $\mathbf{M}_t$ and $\mathbf{S}_t$ are

$$M_{ijt} \equiv \frac{K_{ikt}L_{it}^{\alpha_1(\sigma-1)}w_{it}^{1-\sigma}}{\sum_{l\in\mathcal{N}} K_{lkt}L_{lt}^{\alpha_1(\sigma-1)}w_{lt}^{1-\sigma}}, \quad S_{ijt} \equiv \frac{\mu_{ikt}^{-\theta}W_{it}^{\theta}}{\sum_{l\in\mathcal{N}} \mu_{lkt}^{-\theta}W_{lt}^{\theta}} \tag{35}$$

where

$$K_{ikt} \equiv \left(\frac{\tau_{ik}}{L_{i,t-1}^{\alpha_2}\bar{A}_i L_{kt-1}^{\beta_2}\bar{u}_k} \right)^{1-\sigma} \tag{36}$$

A stationary equilibrium $\mathbf{L}^*$ should satisfy $\boldsymbol{z}(\boldsymbol{w}^*, \mathbf{L}^*, \mathbf{L}^*) = \mathbf{0}$ where $\boldsymbol{w}^*$ is the associated nominal wages.

Let $d\boldsymbol{w}_t$, $d\mathbf{L}_t$, and $d\mathbf{L}_{t-1}$ denote infinitesimal changes, and let $\mathbf{Z}_{ik}$ denote the partial derivative of the function $\boldsymbol{z}_i(\cdot,\cdot,\cdot)$ with respect to its k-th argument. We then obtain the following total differential:

$$\begin{cases} \mathbf{Z}_{11}\, d\boldsymbol{w}_t + \mathbf{Z}_{12}\, d\mathbf{L}_t + \mathbf{Z}_{13}\, d\mathbf{L}_{t-1} = \mathbf{0} \\ \mathbf{Z}_{21}\, d\boldsymbol{w}_t + \mathbf{Z}_{22}\, d\mathbf{L}_t + \mathbf{Z}_{23}\, d\mathbf{L}_{t-1} = \mathbf{0} \end{cases} \tag{37}$$

$$\implies \begin{bmatrix} \mathbf{Z}_{11} & \mathbf{Z}_{12} \\ \mathbf{Z}_{21} & \mathbf{Z}_{22} \end{bmatrix} \begin{bmatrix} d\boldsymbol{w}_t \\ d\mathbf{L}_t \end{bmatrix} = \begin{bmatrix} -\mathbf{Z}_{13} \\ -\mathbf{Z}_{23} \end{bmatrix} d\mathbf{L}_{t-1} \tag{38}$$

$$\implies \begin{bmatrix} d\boldsymbol{w}_t \\ d\mathbf{L}_t \end{bmatrix} = \begin{bmatrix} \mathbf{Z}_{11} & \mathbf{Z}_{12} \\ \mathbf{Z}_{21} & \mathbf{Z}_{22} \end{bmatrix}^{-1} \begin{bmatrix} -\mathbf{Z}_{13} \\ -\mathbf{Z}_{23} \end{bmatrix} d\mathbf{L}_{t-1} \tag{39}$$

The inverse of a 2×2 block matrix is given by:

$$\begin{bmatrix} \mathbf{A} & \mathbf{B} \\ \mathbf{C} & \mathbf{D} \end{bmatrix}^{-1} = \begin{bmatrix} \mathbf{A}^{-1} + \mathbf{Q}\mathbf{C}\mathbf{A}^{-1} & -\mathbf{Q} \\ -\mathbf{P}^{-1}\mathbf{C}\mathbf{A}^{-1} & \mathbf{P}^{-1} \end{bmatrix}, \tag{40}$$

where $\mathbf{P} \equiv \mathbf{D} - \mathbf{C}\mathbf{A}^{-1}\mathbf{B}$ and $\mathbf{Q} \equiv \mathbf{A}^{-1}\mathbf{B}\mathbf{P}^{-1}$, and we assume both $\mathbf{A}$ and $\mathbf{P}$ are invertible.

Applying this result to the second block row of Eq. (39), we obtain:

$$\begin{aligned} d\mathbf{L}_t &= \left(-\mathbf{P}^{-1}\mathbf{C}\mathbf{A}^{-1}\mathbf{Z}_{13} + \mathbf{P}^{-1}\mathbf{Z}_{23}\right) d\mathbf{L}_{t-1} \\ &= \mathbf{P}^{-1}\left(\mathbf{Z}_{23} - \mathbf{C}\mathbf{A}^{-1}\mathbf{Z}_{13}\right) d\mathbf{L}_{t-1} \\ &= \underbrace{\left(\mathbf{Z}_{22} - \mathbf{Z}_{21}\mathbf{Z}_{11}^{-1}\mathbf{Z}_{12}\right)^{-1}\left(\mathbf{Z}_{23} - \mathbf{Z}_{21}\mathbf{Z}_{11}^{-1}\mathbf{Z}_{13}\right)}_{\nabla \mathbf{F}} d\mathbf{L}_{t-1} \end{aligned}$$

Thus, we conclude that

$$\nabla \mathbf{F}(\mathbf{L}^*) = \left(\mathbf{Z}_{22} - \mathbf{Z}_{21}\mathbf{Z}_{11}^{-1}\mathbf{Z}_{12}\right)^{-1}\left(\mathbf{Z}_{23} - \mathbf{Z}_{21}\mathbf{Z}_{11}^{-1}\mathbf{Z}_{13}\right)\Big|_{\mathbf{L}=\mathbf{L}^*} \tag{41}$$

Further, we compute as follows:

$$\begin{aligned} \mathbf{Z}_{11} =& (1-\sigma)\left(\mathbf{M}\hat{\mathbf{Y}}_t\mathbf{M}^\top \hat{\boldsymbol{w}}_t^{-1} - \hat{\mathbf{L}}_t\right) + (\mathbf{I} - \mathbf{M})\hat{\mathbf{L}}_t \\ \mathbf{Z}_{12} =& \alpha_1(\sigma-1)\left(\mathbf{M}\hat{\mathbf{Y}}_t\mathbf{M}^\top \hat{\mathbf{L}}_t^{-1} - \hat{\boldsymbol{w}}_t\right) + (\mathbf{I} - \mathbf{M})\hat{\boldsymbol{w}}_t \\ \mathbf{Z}_{13} =& (1-\sigma)\{\alpha_2\left(\hat{\mathbf{L}}_t\hat{\boldsymbol{w}}_t - \mathbf{M}\hat{\mathbf{Y}}_t\mathbf{M}^\top\right) + \beta_2\left(\mathbf{M}\hat{\mathbf{L}}_t\hat{\boldsymbol{w}}_t - \mathbf{M}\hat{\mathbf{L}}_t\hat{\boldsymbol{w}}_t\hat{\mathbf{L}}_{t-1}\right)\}\hat{\mathbf{L}}_{t-1}^{-1} \\ \mathbf{Z}_{21} =& \theta\left\{\mathbf{S}\hat{\mathbf{L}}_{t-1}\mathbf{S}^\top \boldsymbol{w}_t^{-1}\left(\mathbf{I} - \mathbf{M}^\top\right) - \hat{\boldsymbol{w}}_t^{-1}\left(\mathbf{I} - \mathbf{M}^\top\right)\hat{\mathbf{L}}_t\right\} \\ \mathbf{Z}_{22} =& \mathbf{I} - \theta\left\{\hat{\mathbf{L}}_t^{-1}\left(\alpha_1\mathbf{M}^\top + \beta_1\mathbf{I}\right)\hat{\mathbf{L}}_t - \mathbf{S}\hat{\mathbf{L}}_{t-1}\mathbf{S}^\top\hat{\mathbf{L}}_t^{-1}\left(\alpha_1\mathbf{M}^\top + \beta_1\mathbf{I}\right)\right\} \\ \mathbf{Z}_{23} =& \theta\Big(\mathbf{S}\hat{\mathbf{L}}_{t-1}\mathbf{S}^\top\hat{\mathbf{L}}_{t-1}^{-1}\left(\alpha_2\mathbf{M}^\top + \beta_2\mathbf{I}\right) - \hat{\mathbf{L}}_{t-1}^{-1}\left(\alpha_2\mathbf{M}^\top + \beta_2\mathbf{I}\right)\hat{\mathbf{L}}_t\Big) - \mathbf{S} \end{aligned}$$

where $\hat{\boldsymbol{v}} \equiv \text{diag}[\boldsymbol{v}]$ denotes the diagonal matrix with diagonal element $\boldsymbol{v}$, and $\mathbf{Y}_t \equiv \boldsymbol{w}_t \circ \mathbf{L}_t$ with $\circ$ being the Hadamard product. In the circular four-location space, when local amenities $\bar{A}_i$ and local productivity $\bar{u}_i$ are spatially uniform, the symmetric population distribution

$$\mathbf{L}_t = \mathbf{L}_{t-1} = \bar{\mathbf{L}} = [l, l, l, l] \quad (l \equiv L/4)$$

constitutes a stationary equilibrium.

Let the distance resistance parameters be defined as $r \equiv \tau^{1-\sigma}$ and $s \equiv \mu^{-\theta}$. Under

these definitions, the spatial discount matrices $\mathbf{D}$ and $\mathbf{E}$ are given by:

$$\mathbf{D} = \begin{bmatrix} 1 & r & r^2 & r \\ r & 1 & r & r^2 \\ r^2 & r & 1 & r \\ r & r^2 & r & 1 \end{bmatrix}, \quad \mathbf{E} = \begin{bmatrix} 1 & s & s^2 & s \\ s & 1 & s & s^2 \\ s^2 & s & 1 & s \\ s & s^2 & s & 1 \end{bmatrix}. \tag{42}$$

Let $\bar{\mathbf{D}}$ and $\bar{\mathbf{E}}$ denote the row-normalized versions of $\mathbf{D}$ and $\mathbf{E}$, respectively. Then, the Jacobian matrix of the inter-temporal dynamics at the dispersed equilibrium can be compactly expressed as:

$$\begin{cases} \mathbf{Z}_{11} = \bar{l}\left\{(\mathbf{I} - \bar{\mathbf{D}}) - (1-\sigma)(\mathbf{I} - \bar{\mathbf{D}}^2)\right\}, \\ \mathbf{Z}_{12} = -\bar{w}\left\{(\mathbf{I} - \bar{\mathbf{D}}) - \alpha_1(1-\sigma)(\mathbf{I} - \bar{\mathbf{D}}^2)\right\}, \quad , \\ \mathbf{Z}_{13} = \bar{w}\alpha_2(1-\sigma)(\mathbf{I} - \bar{\mathbf{D}}^2) \end{cases} \tag{43}$$

$$\begin{cases} \mathbf{Z}_{21} = -\theta\frac{\bar{l}}{\bar{w}}(\mathbf{I} - \bar{\mathbf{D}})(\mathbf{I} - \bar{\mathbf{E}}^2), \\ \mathbf{Z}_{22} = \mathbf{I} - \theta(\beta_1\mathbf{I} + \alpha_1\bar{\mathbf{D}})(\mathbf{I} - \bar{\mathbf{E}}^2), \\ \mathbf{Z}_{23} = -\theta(\beta_2\mathbf{I} + \alpha_2\bar{\mathbf{D}})(\mathbf{I} - \bar{\mathbf{E}}^2) - \bar{\mathbf{E}} \end{cases} \tag{44}$$

Since all of the above matrices are symmetric circulant matrices, they share a common set of eigenvectors. Consequently, the k-th eigenvalue of each block in the Jacobian matrix can be expressed using the eigenvalues χ_k and λ_k of $\bar{\mathbf{D}}$ and $\bar{\mathbf{E}}$, respectively, as follows:

$$\begin{cases} \zeta_{1k}^{(1)} = \bar{l}\left\{(1 - \chi_k) - (1-\sigma)(1 - \chi_k^2)\right\}, \\ \zeta_{1k}^{(2)} = -\bar{w}\left\{(1 - \chi_k) - \alpha_1(1-\sigma)(1 - \chi_k^2)\right\}, \\ \zeta_{1k}^{(3)} = \bar{w}\alpha_2(1-\sigma)(1 - \chi_k^2) \end{cases} \tag{45}$$

$$\begin{cases} \zeta_{2k}^{(1)} = -\theta\frac{\bar{l}}{\bar{w}}(1 - \chi_k)(1 - \lambda_k^2), \\ \zeta_{2k}^{(2)} = 1 - \theta(\beta_1 + \alpha_1\chi_k)(1 - \lambda_k^2), \\ \zeta_{2k}^{(3)} = -\theta(\beta_2 + \alpha_2\chi_k)(1 - \lambda_k^2) - \lambda_k \end{cases} \tag{46}$$

Using these expressions, the k-th eigenvalue f_k of the full Jacobian matrix $\nabla\mathbf{L}_t$ can be

written as:

$$f_k = \frac{h_k^\sharp}{h_k^\flat}, \qquad \text{where} \quad \begin{cases} h_k^\sharp = \dfrac{\zeta_{2k}^{(1)}\zeta_{1k}^{(3)}}{\zeta_{1k}^{(1)}} - \zeta_{2k}^{(3)}, \\ h_k^\flat = \zeta_{2k}^{(2)} - \dfrac{\zeta_{2k}^{(1)}\zeta_{1k}^{(2)}}{\zeta_{1k}^{(1)}} \end{cases} . \tag{47}$$

References

Akamatsu, T., Mori, T., Osawa, M., and Takayama, Y. (2017). Spatial scale of agglomeration and dispersion: Theoretical foundations and empirical implications. https://arxiv.org/abs/1912.05113.

Akamatsu, T., Mori, T., Osawa, M., and Takayama, Y. (2024). Spatial scale of agglomeration and dispersion: Number, spacing, and the spatial extent of cities. https://arxiv.org/abs/1912.05113.

Allen, T. and Arkolakis, C. (2014). Trade and the topography of the spatial economy. *The Quarterly Journal of Economics*, pages 1085–1139.

Allen, T. and Donaldson, D. (2020). Persistence and path dependence in the spatial economy. Technical report, National Bureau of Economic Research.

Allen, T. and Donaldson, D. (2022). Persistence and path dependence: A primer. *Regional Science and Urban Economics*, 94:103724.

Armington, P. S. (1969). A theory of demand for products distinguished by place of production. *Staff Papers of International Monetary Fund*, pages 159–178.

Behrens, K. and Murata, Y. (2021). On quantitative spatial economic models. *Journal of Urban Economics*, 123:103348.

Fujita, M. and Thisse, J.-F. (2013). *Economics of Agglomeration: Cities, Industrial Location, and Regional Growth, 2nd Edition*. Cambridge university press.

Helpman, E. (1998). The size of regions. In Pines, D., Sadka, E., and Zilcha, I., editors, *Topics in Public Economics*, pages 33–54. Cambridge University Press Cambridge.

Hornbeck, R., Michaels, G., and Rauch, F. (2024). Identifying agglomeration shadows: Long-run evidence from ancient ports. Technical report, National Bureau of Economic Research.

Ikeda, K., Akamatsu, T., and Kono, T. (2012). Spatial period-doubling agglomeration of a core–periphery model with a system of cities. *Journal of Economic Dynamics and Control*, 36(5):754–778.

Krugman, P. (1991). Increasing returns and economic geography. *Journal of Political Economy*, 99(3):483–499.

Krugman, P. (1993). First nature, second nature, and metropolitan location. *Journal of Regional Science*, 33(2):129–144.

Matsuyama, K. (2017). Geographical advantage: Home market effect in a multi-region world. *Research in Economics*, 71(4):740–758.

Proost, S. and Thisse, J.-F. (2019). What can be learned from spatial economics? *Journal of Economic Literature*, 57(3):575–643.

Sugimoto, T., Takayama, Y., and Takagi, A. (2025). A quantitative spatial model for evaluating transport-induced spatial reorganization. *Transport Policy*, 172:103738.